Effects of Dimensional Crossover on Flux Pinning in a Model High-T_c Superconductor: $YBa_2Cu_3O_{7-\delta}/(Pr_xY_{1-x})Ba_2Cu_3O_{7-\delta}$ Superlattices

Qi Li, C. Kwon, X. X. Xi, S. Bhattacharya, A. Walkenhorst, T. Venkatesan,[a] S. J. Hagen, W. Jiang, and R. L. Greene

Center for Superconductivity Research, Department of Physics, University of Maryland, College Park, Maryland 20742

(Received 5 June 1992)

Superlattices of one-unit-cell-thick $YBa_2Cu_3O_{7-\delta}$ layers with $(Pr_xY_{1-x})Ba_2Cu_3O_{7-\delta}$ were fabricated as a model system to study the effects of magnetic coupling on flux pinning in high-T_c superconductors. The sample can be transformed from an S/S′ to an S/N structure by increasing the temperature from below to above the T_c of the intercalating $(Pr_xY_{1-x})Ba_2Cu_3O_{7-\delta}$ layer. Dramatic changes in the characteristics of the magnetic field and angle dependence of the critical current density, $J_c(B,\Theta)$, caused by a 3D to 2D crossover were observed. The result demonstrates the significance of the dimensionality to the flux pinning in these materials with layered structures.

PACS numbers: 74.60.Ge, 74.60.Jg, 74.70.Jm, 74.75.+t

The vortex structure and vortex motion in the highly anisotropic high-T_c superconductors have been extensively studied in recent years. The mechanism of pinning and the effect of anisotropy are among the central issues [1]. The degree of anisotropy and pinning varies among the cuprates. A model proposed by Tachiki and Takahashi emphasizes the extrinsic planar pinning such as twin planes [2], and could fit the experimental data of angle dependence of the critical current density, $J_c(\Theta)$, in $YBa_2Cu_3O_{7-\delta}$ (YBCO) at high fields [3]. On the other hand, the scaling behavior of magnetic field and angle dependence, $J_c(B,\Theta)$, in $Bi_2Sr_2CaCu_2O_{8+x}$ (BSCCO) [4] has been interpreted by a two-dimensional model suggested by Kes *et al.* [5]. Recently, Hao and Clem [6] and Blatter, Geshkenbein, and Larkin [7] proposed that scaling properties exist in anisotropic superconductors which can also explain the behavior of $J_c(B,\Theta)$ in BSCCO. Since the microstructures of different cuprate superconductors differ, a comparison among them may not clarify the role of magnetic interplanar coupling and pinning in these materials.

In this Letter, we report measurements of $J_c(B,\Theta)$ in a model high-T_c superconductor: *c*-axis-oriented $YBa_2Cu_3O_{7-\delta}/(Pr_xY_{1-x})Ba_2Cu_3O_{7-\delta}$ superlattices, in which the interplanar coupling can be manipulated while the microscopic structure of the pinning centers remains unchanged. Each YBCO layer in the superlattices contains only one CuO_2 double plane, the building block of YBCO and many other high-T_c materials. However, the coupling between them is determined by the properties of the $(Pr_xY_{1-x})Ba_2Cu_3O_{7-\delta}$ [(Pr_xY_{1-x})BCO] layers intercalated between them, which can vary from nearly insulating to superconducting depending on the doping level. By properly choosing x, the (Pr_xY_{1-x})BCO layers can have a transition temperature $T_c^{\rm int}$ lower than that of the YBCO layer and consequently, the structure can be switched from an S/S′ to an S/N superlattice by varying the temperature from below to above $T_c^{\rm int}$.

The superlattice samples were grown on (100) $SrTiO_3$ substrates by pulsed laser deposition. The details of sample preparation and characterization have been published earlier [8,9] and also reported by other groups [10–15]. The YBCO layer thickness was 1.2 nm and the (Pr_xY_{1-x})BCO layer thickness was 9.6 nm (1.2 nm for the sample with $x=1$). The samples were patterned using standard lithography into 20 μm×100 μm bridges. The *I-V* curves were measured as a function of magnetic field B, temperature T, and the angle of the magnetic field with respect to the c axis, Θ. The measurement current was always perpendicular to the magnetic field. The J_c is defined using a voltage criterion of 1 μV and calculated using the total film thickness (including the nonsuperconducting layers), which will give lower values than the actual J_c of the superconducting layers in some cases. The angular position was calibrated and determined by a standard thin-film Hall sensor placed parallel to the sample surface, giving an angular precision better than a few tenths of a degree.

The parameters of the three superlattice samples described in this paper are summarized in Table I. $T_c(R=0)$ represents the zero-resistance temperature of the superlattices and $T_c^{\rm int}(R=0)$ represents that of a 50-nm-thick (Pr_xY_{1-x})BCO film made under identical conditions. The main results presented are from sample 1 ($x=0.4$) with a T_c of 74 K; the $T_c^{\rm int}$ of the $(Pr_{0.4}Y_{0.6})$BCO film is 50 K. The T_c of this sample is higher than that in superlattices with PrBCO intercalating layers [8,10–12]. We have found that the T_c of unit-cell-thick YBCO depends strongly on the properties of the layers adjacent to it, a detailed study of which will be published separately [9]. We could not measure directly the T_c of the $(Pr_{0.4}Y_{0.6})$BCO layers in the superlattice but it is anticipated to be similar to the thick-film value due to the layer thickness used. The results for samples with $x=0.1$ (sample 2) and $x=1$ (sample 3) are presented for comparison with sample 1.

In Fig. 1, J_c of sample 1 as a function of B is plotted for two field directions, $\mathbf{B}\perp(a,b)$ planes and $\mathbf{B}\parallel(a,b)$ planes, at (a) $T<T_c^{\rm int}$ ($T=25$ K) and (b) $T>T_c^{\rm int}$ ($T=52$ K). In Fig. 1(a), the sample is of an S/S′ structure

TABLE I. Parameters of YBCO/(Pr_xY_{1-x})BCO superlattice samples used in this work. d_{YBCO} is the thickness of YBCO layer and d_{int} is that of the intercalating (Pr_xY_{1-x})BCO layer. $T_c(R=0)$ and $T_c^{int}(R=0)$ are the zero-resistance temperatures of the superlattice and the intercalating layer, respectively.

Sample	Intercalation layer	d_{YBCO} (nm)	d_{int} (nm)	$T_c(R=0)$ (K)	$T_c^{int}(R=0)$ (K)	Number of periods
1	$x=0.4$	1.2	9.6	74	50	18
2	$x=0.1$	1.2	9.6	87	81	18
3	$x=1$	1.2	1.2	75	Insulating	65

and the $J_c(B)$ curve is very similar to the result for a thick YBCO film [3] [see Fig. 1(b)]. With $\mathbf{B}\perp(a,b)$, J_c drops fast at low field but changes much more slowly at high field. For $T>T_c^{int}$, the $J_c(B)$ behavior is dramatically different: For $\mathbf{B}\perp(a,b)$, J_c drops much more rapidly and $\log(J_c)$ falls almost linearly with B throughout the field range. When $\mathbf{B}\parallel(a,b)$, J_c changes weakly with magnetic field. The $J_c(B)$ curves for a 2000-Å YBCO film at the same reduced temperature ($T=60$ K, $t=T/T_c=0.67$) are also plotted for comparison. As seen in Fig. 1(b), the $J_c(B)$ curves of the superlattice are very different from that of the thick YBCO film. Instead, this field dependence is very similar to the results for BSCCO which have been attributed to the weaker pinning in the material. In our case, the microstructure and thus the pinning centers are identical for Figs. 1(a) and 1(b). The only difference is a weakened coupling between the YBCO unit cells since the sample is switched from an S/S′ to an S/N structure.

The Θ dependence of J_c of sample 1 at $T<T_c^{int}$ is shown in Fig. 2(a) for two magnetic field values. The symbols are the measurement data and the lines are calculated from the relation

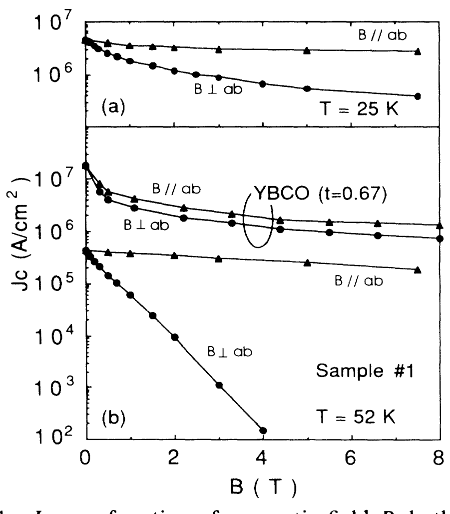

FIG. 1. J_c as a function of magnetic field B, both $\mathbf{B}\perp(a,b)$ and $\mathbf{B}\parallel(a,b)$, for sample 1 at (a) $T=25$ K ($T<T_c^{int}$) and (b) $T=52$ K ($T>T_c^{int}$). In (b), the result for a YBCO film at 60 K (the same reduced temperature $t=0.67$) is also plotted for comparison.

$$J_c(\Theta)=J_{c\perp}/(\cos\Theta)^{1/2} \qquad (1)$$

derived by Tachiki and Takahashi [2] to explain the results in YBCO, where $J_{c\perp}$ is the J_c value when $\mathbf{B}\perp(a,b)$. In this model, when a magnetic field is applied to an angle Θ, the vortex lines are stepwise with segments along and normal to the a-b planes due to the layered structure in YBCO. The motion of the vortex line segments perpendicular to the a-b plane dominates the dissipation in YBCO. The pinning of these vortex line segments (the portion of which is determined by $B\cos\Theta$) by extrinsic pinning centers, such as planar defects, determines $J_c(\Theta)$ until it reaches $J_{c\parallel}$, the J_c value for $\mathbf{B}\parallel(a,b)$, which is

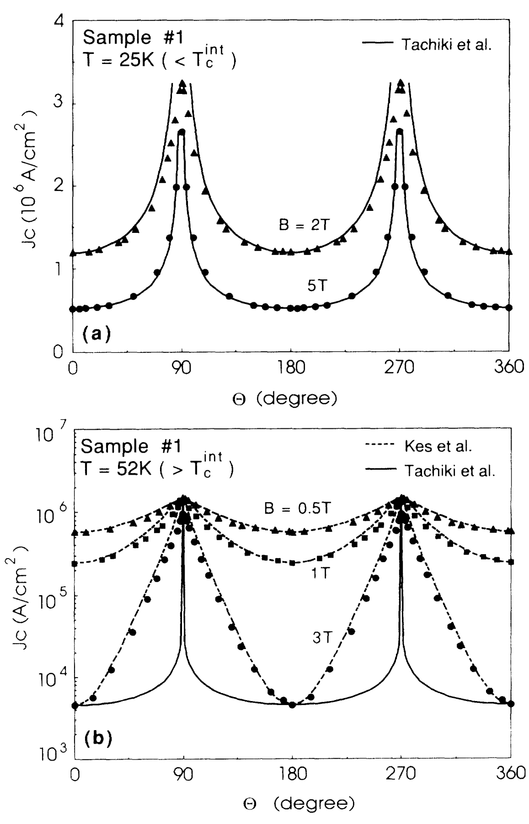

FIG. 2. Angular dependence of J_c for sample 1 at (a) $T=25$ K ($T<T_c^{int}$) and (b) $T=52$ K ($T>T_c^{int}$). Also plotted are the calculated curves from Eq. (1) by Tachiki and Takahashi (solid lines) and from Eq. (2) by Kes *et al.* (dashed lines).

determined by the intrinsic pinning [16]. As shown in Fig. 2, the model fits the experimental data very well at high field, indicating a similar vortex line configuration to that in YBCO.

The $J_c(\Theta)$ curves of sample 1 for $T > T_c^{\rm int}$ are shown in Fig. 2(b) for several field values. The symbols are the experimental data and the dashed lines are calculated using the scaling relation of a 2D model proposed by Kes *et al.* [5],

$$J_c(B,\Theta) = J_{c\perp}(B\cos\Theta, 0) . \quad (2)$$

The $J_{c\perp}(B,0)$ function used for calculating $J_c(B,\Theta)$ was taken from the experimental data as shown in Fig. 1(b). The result of Eq. (1) for $B = 3$ T is also plotted for comparison. It is clearly shown that at this temperature, when the sample is of an S/N structure, Eq. (1) fails to explain the experimental results whereas the model by Kes *et al.* fits the $J_c(\Theta)$ data very well for all fields. This model proposes that when the conducting planes are very weakly coupled the magnetic field parallel to the planes penetrates between these planes uniformly. Therefore, when a magnetic field is applied at an angle Θ, only the $B_\perp = B\cos\Theta$ component will contribute to dissipation.

In order to rule out the possibility that the change of $J_c(B,\Theta)$ behavior at $T > T_c^{\rm int}$ is a temperature effect, we measured sample 2 at the same temperature as in Fig. 2(b) and the results are shown in Fig. 3. In sample 2, the intercalating $(Pr_{0.1}Y_{0.9})$BCO layer has a higher $T_c^{\rm int}$ (81 K), and therefore at 52 K the sample is still of an S/S′ structure. Comparing Fig. 3 with Fig. 2(b), one finds that even at the same temperature, $J_c(\Theta)$ of an S/S′ structure can be fitted by Eq. (1) at high fields while that of an S/N structure is better described by Eq. (2). This indicates that the different angular dependence of J_c at $T > T_c^{\rm int}$ for sample 1 is not simply due to the higher measurement temperature.

The different $J_c(B,\Theta)$ dependences of sample 1 below and above $T_c^{\rm int}$ are rather due to a crossover of the sample

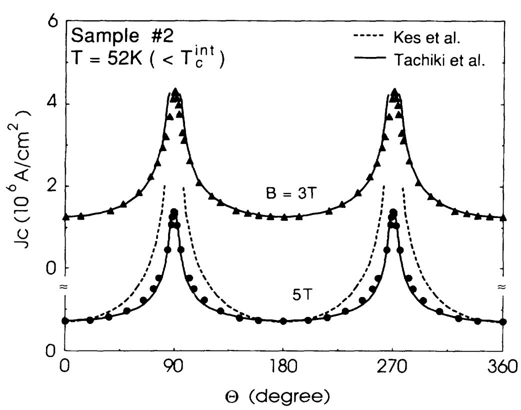

FIG. 3. Angular dependence of J_c for sample 2 at $T = 52$ K, the same temperature as in Fig. 2(b). Because of the different doping in the (Pr_xY_{1-x})BCO layer, $T < T_c^{\rm int}$ in this case.

from anisotropic 3D to 2D behavior. When $T < T_c^{\rm int}$ the $(Pr_{0.4}Y_{0.6})$BCO layer is superconducting which mediates the coupling between the neighboring YBCO layers in terms of forming magnetic vortex lines. As T is increased to above $T_c^{\rm int}$, however, the superconducting order parameter in the $(Pr_{0.4}Y_{0.6})$BCO layer becomes zero (assuming that the layer thickness of 9.6 nm is much larger than the proximity coherence length in the c direction), and hence decouples these YBCO planes. Since both S/N and S/S′ structures are realized in the same sample, the effects of pinning centers in the plane and the dimensionality are clearly separated.

Based on the original assumption of planar pinning in Tachiki and Takahashi's model, Eq. (1) should still be valid for our S/N structure since no structure change has taken place. The failure of using Eq. (1) to explain $J_c(\Theta)$ at $T > T_c^{\rm int}$ indicates that the interplanar coupling and dimensionality play more important roles than the microstructure of pinning centers in determining the angular dependence of J_c.

With respect to the field dependence, J_c drops substantially faster with increasing magnetic field when the CuO_2 double planes are decoupled. In this case, a continuous vortex is broken into a series of 2D pancakes [17]. Currently, the defects considered to be the pinning centers in YBCO include oxygen vacancies (point defects) and edge and screw dislocations (planar defects). Since the density of point defects in YBCO is high and each point defect only pins a small length of vortex line (tens of angstroms) [1], most pieces of the broken vortex lines still interact with almost the same number of point defects. Pinning by the planar defects also should not change when the vortex lines are broken. The J_c value of 2×10^6 A/cm^2 at 4.2 K was obtained in our single one-unit-cell-thick YBCO layer despite its T_c of 43 K, which proves the theoretical estimation [1] that a high density of pinning sites is present in each unit-cell layer of YBCO films. Recent results showed that the characteristics of the thermal activation energy $U_0(B)$ are different for a single and a coupled $Mo_{77}Ge_{23}$ multilayer [18]. Our results also indicate that when the sample is switched from 3D to 2D, the functional dependence of pinning energy on B is changed.

It is worth noticing that with the microstructure, hence the pinning centers, being the same, the $J_c(B,\Theta)$ behavior is switched from YBCO-like at $T < T_c^{\rm int}$ to BSCCO-like at $T > T_c^{\rm int}$ just by decoupling the CuO_2 double planes. This is consistent with the suggestion that the difference between YBCO and BSCCO in terms of vortex pinning is in the interplanar coupling, while our result is the first to demonstrate unambiguously the significant effect of dimensionality on the flux pinning in high-T_c superconductors.

The effect of dimensionality on the critical current behavior is also confirmed in a sample with $x = 1$ (sample 3). Figure 4(a) shows the $J_c(\Theta)$ dependence of a

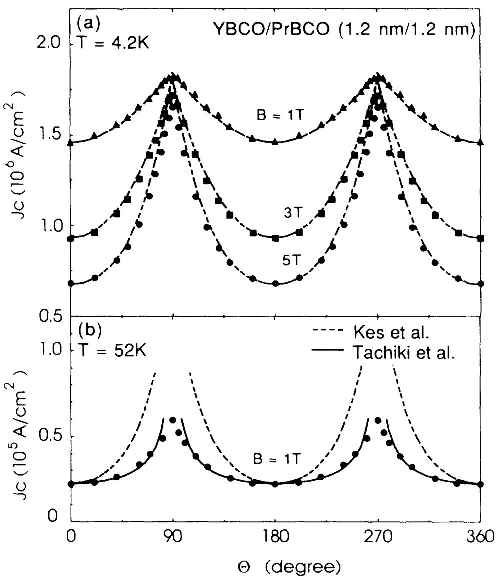

FIG. 4. Angular dependence of J_c for sample 3, a (1.2 nm)/(1.2 nm) YBCO/PrBCO superlattice, at (a) $T=4.2$ K and (b) $T=52$ K.

YBCO/PrBCO [(1.2 nm)/(1.2 nm)] superlattice at 4.2 K for different fields. As seen in the figure, $J_c(B,\Theta)$ can be described by the 2D model [Eq. (2)], indicating that one-unit-cell-thick PrBCO is already sufficient to decouple the adjacent YBCO layers at 4.2 K [for this sample at 4.2 K, the difference between the results from Eqs. (1) and (2) is small]. Similar results have also been observed in a (2.4 nm)/(1.2 nm) YBCO/PrBCO superlattice by Jakob *et al.* [19]. Contrary to the situation described above in Fig. 2, the coupling between the YBCO layers in sample 3 becomes stronger with increasing temperature due to the change of the coherence length [20]. Indeed, the $J_c(\Theta)$ of sample 3 deviated from the 2D model at high temperatures as shown in Fig. 4(b) ($T=52$ K), and Eq. (1) gives a better fit to the data again. It should be noted that the crossover temperature we observed is much lower than that estimated from Ref. [5]. We have also observed that at $T=52$ K, the 2D model becomes appropriate and Eq. (1) fails again at higher magnetic fields ($B=5$ T). This may indicate that the crossover temperature from 3D to 2D depends on the magnetic field as well, as proposed by Vinokur *et al.* [21].

In conclusion, YBCO/(Pr_xY_{1-x})BCO superlattices were used as a model system to study the effects of interplanar coupling and pinning centers on the vortex pinning in high-T_c superconductors. The coupling between CuO_2 double planes was manipulated without changing the microstructure of the samples by varying the temperature with respect to T_c^{int}. When the CuO_2 planes changes from coupled to decoupled, characteristic changes in the behavior of $J_c(B)$ and $J_c(\Theta)$ were observed. We conclude that the interplanar coupling is a very important parameter in determining the flux motion in high-T_c superconductors.

The authors would like to thank P. H. Kes, J. R. Clem, C. J. Lobb, D. Wu, and S. Anlage for very helpful discussions and J. L. Peng, Z. Y. Li, and X. Xu for experimental assistance.

---

[a] Also with the Department of Electrical Engineering.

[1] See, for example, P. H. Kes in "Phenomenology and Applications of High Temperature Superconductors" (to be published); A. P. Malozemoff, Physica (Amsterdam) **185C**, 264 (1991).
[2] M. Tachiki and S. Takahashi, Solid State Commun. **72**, 1083 (1989).
[3] B. Roas *et al.*, Phys. Rev. Lett. **64**, 479 (1990).
[4] P. Schmitt *et al.*, Phys. Rev. Lett. **67**, 267 (1991).
[5] P. H. Kes *et al.*, Phys. Rev. Lett. **64**, 1063 (1990).
[6] Z. Hao and J. R. Clem, Phys. Rev. B **46**, 5853 (1992).
[7] G. Blatter, V. B. Geshkenbein, and A. I. Larkin, Phys. Rev. Lett. **68**, 875 (1992).
[8] Q. Li *et al.*, Phys. Rev. Lett. **64**, 3086 (1990).
[9] C. Kwon *et al.* (unpublished).
[10] J.-M. Triscone *et al.*, Phys. Rev. Lett. **64**, 804 (1990).
[11] D. H. Lowndes *et al.*, Phys. Rev. Lett. **65**, 1160 (1990).
[12] D. P. Norton *et al.*, Phys. Rev. Lett. **67**, 1358 (1991).
[13] T. Terashima *et al.*, Phys. Rev. Lett. **67**, 1362 (1991).
[14] S. J. Pennycook *et al.*, Phys. Rev. Lett. **67**, 765 (1991).
[15] O. Brunner *et al.*, Phys. Rev. Lett. **67**, 1354 (1991).
[16] M. Tachiki and M. Takahashi, Solid State Commun. **70**, 291 (1989); B. I. Ivlev and N. B. Kopnin, Phys. Rev. Lett. **64**, 1828 (1990); D. Feinberg and C. Villard, Phys. Rev. Lett. **65**, 919 (1990).
[17] J. R. Clem, Phys. Rev. B **43**, 7837 (1990).
[18] W. R. White *et al.*, Phys. Rev. Lett. **66**, 2826 (1991).
[19] G. Jakob *et al.*, Appl. Phys. Lett. **59**, 1626 (1991).
[20] W. E. Lawrence and S. Doniach, in *Proceedings of the Twelfth International Conference on Low Temperature Physics, Kyoto, 1970*, edited by E. Kanda (Keigaku, Tokyo, 1971), p. 361.
[21] V. M. Vinokur *et al.*, Physica (Amsterdam) **168C**, 29 (1990).